Published in final edited form as:
Plant Mol Biol. 2012 September ; 80(1): 117–129. doi:10.1007/s11103-011-9778-9.

An autoregulatory feedback loop involving *PAP1* and *TAS4* in response to sugars in Arabidopsis

Qing-Jun Luo, **Amandeep Mittal**, **Fan Jia**, and **Christopher D. Rock**
Department of Biological Sciences, Texas Tech University, Lubbock, TX 79409-3131, USA

Christopher D. Rock: chris.rock@ttu.edu

Abstract

miR828 in Arabidopsis triggers the cleavage of *Trans-Acting SiRNA Gene 4* (*TAS4*) transcripts and production of small interfering RNAs (*ta*-siRNAs). One siRNA, *TAS4*-siRNA81(−), targets a set of MYB transcription factors including *PAP1, PAP2*, and *MYB113* which regulate the anthocyanin biosynthesis pathway. Interestingly, miR828 also targets MYB113, suggesting a close relationship between these MYBs, miR828, and *TAS4*, but their evolutionary origins are unknown. We found that *PAP1, PAP2*, and *TAS4* expression is induced specifically by exogenous treatment with sucrose and glucose in seedlings. The induction is attenuated in abscisic acid (ABA) pathway mutants, especially in *abi3-1* and *abi5-1* for *PAP1* or *PAP2*, while no such effect is observed for *TAS4. PAP1* is under regulation by *TAS4*, demonstrated by the accumulation of *PAP1* transcripts and anthocyanin in *ta*-siRNA biogenesis pathway mutants. *TAS4*-siR81(−) expression is induced by physiological concentrations of Suc and Glc and in *pap1-D*, an activation-tagged line, indicating a feedback regulatory loop exists between *PAP1* and *TAS4*. Bioinformatic analysis revealed *MIR828* homologues in dicots and gymnosperms, but only in one basal monocot, whereas *TAS4* is only found in dicots. Consistent with this observation, *PAP1, PAP2*, and *MYB113* dicot paralogs show peptide and nucleotide footprints for the *TAS4-siR81*(−) binding site, providing evidence for purifying selection in contrast to monocots. Extended sequence similarities between *MIR828, MYBs*, and *TAS4* support an inverted duplication model for the evolution of *MIR828* from an ancestral gymnosperm *MYB* gene and subsequent formation of *TAS4* by duplication of the miR828* arm. We obtained evidence by modified 5′-RACE for a *MYB* mRNA cleavage product guided by miR828 in *Pinus resinosa*. Taken together, our results suggest that regulation of anthocyanin biosynthesis by *TAS4* and miR828 in higher plants is evolutionarily significant and consistent with the evolution of *TAS4* since the dicot—monocot divergence.

Keywords

PAP1; TAS4; miR828; Sugar response; Feedback regulation; *TAS* evolution

Introduction

Trans-Acting SiRNA (*TAS*) genes are small interfering RNA (siRNA)-generating loci that regulate target gene expression in *trans* (Peragine et al. 2004; Vazquez et al. 2004; Allen et

Correspondence to: Christopher D. Rock, chris.rock@ttu.edu.

Present Address: Q.-J. Luo, Department of Pediatrics, Stanford University, Stanford, CA 94305-5208, USA

Electronic supplementary material The online version of this article (doi:10.1007/s11103-011-9778-9) contains supplementary material, which is available to authorized users.

al. 2005). The production of *trans*-acting siRNAs (*ta*-siRNAs) from *TAS* loci depends on microRNA (miRNA)-directed cleavage of their transcripts by ARGONAUTE (AGO)-containing RNA-Induced Silencing Complexes (RISCs), which sets the phase for 21-nt siRNA production by RNA-DEPENDENT RNA POLYMERASE 6 (RDR6) in collaboration with SUPPRESSOR OF GENE SILENCING 3 (SGS3), DICER-LIKE 4 (DCL4), DOUBLE-STRANDED RNA BINDING PROTEIN 4 (DRB4), and HUA ENHANCER 1 (HEN1), a small RNA (sRNA) methyltransferase (Peragine et al. 2004; Vazquez et al. 2004; Allen et al. 2005; Yoshikawa et al. 2005). *Arabidopsis thaliana* has eight *TAS* loci from four families, *TAS1-4* (Allen et al. 2005; Rajagopalan et al. 2006). *TAS1* and *TAS2* transcripts are subject to miR173-directed cleavage in association with AGO1 to generate siRNAs targeting several transcripts of pentatricopeptide repeat-containing genes and others with unknown function (Allen et al. 2005; Montgomery et al. 2008b). *TAS3* transcript, on the other hand, is cleaved through the specific interaction of miR390 with AGO7 (Adenot et al. 2006; Fahlgren et al. 2006; Garcia et al. 2006; Montgomery et al. 2008a). Interestingly, an autoregulatory network has been found involving miR390, *TAS3*, and *ta*-siRNA targets *AUXIN RESPONSE FACTORS 2* (*ARF2*), *ARF3*, and *ARF4* (Yoon et al. 2010; Marin et al. 2010). *TAS3*-derived siRNAs (*ta*-siARFs) inhibit *ARF2/3/4* expression, while *ARF4* downregulates miR390 accumulation in contrast to the upregulation of miR390 by *ARF3* in response to auxin. The outcome of this complex feedback loop is a fine-tuning of lateral root growth dependent on the auxin receptor TRANSPORT INHIBITOR RESPONSE 1 (TIR1; a target of miR393), which directs transcriptional regulation in response to localized auxin fluxes (Yoon et al. 2010; Marin et al. 2010).

Regulatory networks of sRNAs, including miRNAs and *ta*-siRNAs, modulate their targets' expression in response to primary (N, P, K) and secondary (S, Mg, Ca) macronutrient condition changes in the cell and/or environment. For example, low sulfate induces miR395 expression, which decreases the mRNA level for its targets *ATP SULFURYLASE 1* (APS1) and several other genes in the sulfate assimilation pathway (Jones-Rhoades and Bartel 2004; Kawashima et al. 2009). The induction of miR395 is modulated by SULFUR LIMITATION 1 (SLIM1), a putative transcription factor in the same pathway, although the expression domain for such induction does not correlate with one of its targets, SULFATE TRANSPORTER 2;1 (SULTR2;1)/ARABIDOPSIS SULFATE TRANSPORTER 68 (AST68) (Kawashima et al. 2009). Other examples include phosphate (P_i) starvation, which up-regulates miR399b/c/f expression and downregulates their common target *PHOSPHATE 2 (PHO2)/UBIQUITIN-CONJUGATING ENZYME 24* (*UBC24*) (Fujii et al. 2005; Chiou et al. 2006). Transgenic Arabidopsis plants over-expressing *MIR399* accumulate five to six times more P_i in shoots than wild type. Intriguingly, a non-coding RNA, *INDUCED BY PHOSPHATE STARVATION 1* (*IPS1*) can sequester miR399 by base-pairing through a mechanism termed "target mimicry" and thereby up-regulate *PHO2* expression level to help translocate over-accumulated P_i in shoots (Franco-Zorrilla et al. 2007). Deep sequencing techniques have uncovered miRNAs such as miR398, miR778, miR827, and miR2111 responsive to P_i deficiency (Pant et al. 2009; Hsieh et al. 2009). Several members of the miR169 family and miR398a are repressed by nitrogen (N) limitation (Pant et al. 2009). Another nutrient-responsive example for miRNAs comes from the report that exogenous sucrose (Suc) treatment increases levels of miR398 in a dose-dependent, but not time-dependent manner, probably by activating the transcription of *MIR398c* (Dugas and Bartel 2008). miR398 reduces the expression of its targets, including *COPPER SUPEROXIDE DISMUTASE 1* (*CSD1*) and *CSD2* at both mRNA and protein levels.

PRODUCTION OF ANTHOCYANIN PIGMENT 1 (PAP1)/MYB DOMAIN PROTEIN 75 (*MYB75*) and *PAP2/MYB90* encode transcription factors that regulate expression of anthocyanin biosynthetic genes in vegetative tissues. They might be involved in regulating

leaf senescence because for both of these processes, sugars can be triggers (Pourtau et al. 2006; Borevitz et al. 2000; Teng et al. 2005; Solfanelli et al. 2006; Gonzalez et al. 2008). In this study, we report that *TAS4* and its targets *PAP1* and *PAP2* are responsive to Suc. Part of the response is impaired in *ABA insensitive 3* (*abi3*) and *abi5* mutants. *PAP1* and *TAS4* expression appear to involve in an autoregulatory loop, as evidenced by the over-accumulation of *PAP1* transcript levels and anthocyanin in *ta*-siRNA pathway mutants, and the up-regulation of *TAS4*-siR81(−) in *pap1-D*, an activation-tagged transgenic line. We also performed bioinformatic analysis and uncovered the existence of miR828 in gymnosperms and angiosperms, whereas *TAS4* only is found in dicots. The cleavage by miR828 was mapped on one MYB transcript from *Pinus resinosa* by 5′-RACE. Finally, sequence alignments suggest an inverted duplication model for *MIR828* and *TAS4* evolution.

Materials and methods

Plant materials and growth conditions

Arabidopsis (*Arabidopsis thaliana* ecotype Columbia) wild-type and mutant plants were grown as previously described (Luo et al. 2009). The accessions used in this study are listed as follows: Ler-0 [CS20], *abi1-1* [CS22], *abi2-1* [CS23], *abi3-1* [CS24], *abi5-1* [CS8105], *aba1-1* [CS21], Col-0 [CS60,000], *abi4-103* [CS3838], *hen1-1* [CS6583], dcl4-2 [CS6954], *drb4* [SALK_113384c], *rdr6-15, sgs3-14* [SALK_001394], *tas4* [SALK_066997], *mir828* [SALK_097788], *hyl1-2* [SALK_064863], *hst-6* [CS24279], *hst-7* [CS24280], and *pap1-D* [CS3884] (Borevitz et al. 2000; Alonso et al. 2003).

For the treatment with sugars, 3-day-old Arabidopsis seedlings were grown on filter papers supplemented with Murashige and Skoog standard medium (MS medium, one-half strength, control). Half of the samples were transferred to new filter papers supplemented with Suc, glucose (Glc) or mannitol solutions at a concentration of 100 mM and harvested by freezing in liquid N_2 at various time points up to 24 h, or subjected to the treatment of different sugars for 12 h with a series of concentrations ranging from 0 to 100 mM.

Taxus globosa (Mexican yew) and *Pinus resinosa* (red pine) plants were purchased from Forrest Farm(Williams, OR) and Heronswood Nursery (Warminster, PA), respectively, and total RNA was extracted from green needles as described (Chang et al. 1993) for Rapid Amplification of cDNA Ends (RACE) experiments.

RNA preparation and detection

Total RNA was isolated using Trizol regent (Invitrogen, Carlsbad CA). Northern blots and sRNA blots were performed as described (Xie et al. 2005). High molecular weight RNA was precipitated from total RNA with 2 M LiCl followed by centrifugation (13,000 rpm, 15 min). The supernatant was added to three volumes 100% ethanol to precipitate low molecular weight RNA. Ten μg total RNA or 20 μg low molecular weight RNA was loaded in each lane for formaldehyde-agarose or PAGE gel electrophoresis, respectively. For Northern blots, probes were prepared from agarose gel-purified *PAP1* cDNA from Arabidopsis cDNA library amplified using primers “PAP1_atgF” and “PAP1_tagR” and radio-labeled with α-^{32}P-dCTP by a random primer labeling kit (Takara, Shiga Japan). To check equal loading, the membrane blot was stripped and re-probed with antisense γ-^{32}P-labelled oligonucleotides for miR160, 5S rRNA, and/or U6 small nuclear RNA (snRNA). RNA blots were scanned using a Storm 860 PhosphorImager (GE Healthcare, Piscataway NJ). mRNA or sRNA signals were quantified using the ImageQuant TL software (v2003, GE Healthcare). Specifically, we divided the *TAS4*-siR81(−), *PAP1*, and control (5S rRNA, miR160, or U6 snRNA) band areas into nine vertical subsections of equal area per lane. The

paired subsections for signals of a given lane were integrated separately after subtracting representative background fields flanking the test and control bands. A ratio of *TAS4*-siR81(−) or *PAP1* mRNA signals to various controls was calculated for these independent sections. The average of four to six uniform ratios across the band was calculated after discarding subsections that contained artifacts identified visually and attributed to gel or blotting processes. Modified RACE experiments were performed according to the manufacturer's specification (Invitrogen). Cloned cDNAs encoding MYB homologues obtained from RACE experiments on *P. resinosa* and *T. globosa* were submitted to GenBank (accession numbers HQ997774 and HQ997775, respectively). Probe and primer sequences are listed in Supplementary Table S1.

Real-time RT-PCR

RNA was extracted from seedlings grown on 0.59× MS medium (control) or on the same medium with 100 mM sugars added for a series of time points as described in Figure legends. Total RNA was subjected to DNase I treatment (Promega, Madison WI) after extraction by Trizol solution (Invitrogen). Five micrograms of each sample were reverse-transcribed into cDNA with Oligo dT primers (Promega) by Moloney Murine Leukemia Virus Reverse Transcriptase (Promega) for 1 h at 42°C. Quantitative real-time PCR (qRT-PCR) assay was performed with the Absolute SYBR Green qPCR Mixes (Thermo Scientific) on the ABI Prism 7,300 sequence detection system (Applied Biosystems, Carlsbad CA). Oligonucleotides were synthesized by Sigma–Aldrich (St. Louis, MO). *ACTIN8* primer pairs were used for internal control on aliquots of cDNA. Relative quantitation for gene expression was done using the comparative CT method as described in the ABI Prism 7300 Sequence Detection System User Bulletin (Applied Biosystems).

Anthocyanin quantitation

Extraction and quantification of anthocyanin from Arabidopsis seedling was performed as described (Teng et al. 2005; Solfanelli et al. 2006) with minor modifications. In brief, 10–20 three day-old seedlings were placed in a microcentrifuge tube and centrifuged briefly to allow surface liquid to be pipetted off. The samples were weighed twice on an analytical balance to obtain an average fresh weight of tissue. One mL of extraction buffer (1% [v/v] hydrochloric acid in methanol) was added followed by incubation at 4°C for 24 h. Extracts were centrifuged (15 min at 13,000 rpm) and the absorbance of the supernatant was determined at 530 and 657 nm in a BioMate 5 spectrophotometer (Thermo Spectronic). Relative anthocyanin units are defined as equal to one absorbance unit $[A_{530} - (1/4 \times A_{657})] \times 1{,}000]$ per gram fresh material in one mL of extraction buffer. Mean values were obtained from three biological replicates.

Bioinformatic analysis

Expressed Sequence Tags (ESTs) and protein sequences were obtained by BLASTing from GenBank (www.ncbi.nlm.nih.gov). The alignment was performed with the Vector NTI software package (Invitrogen, Version 9) or T-Coffee (www.tcoffee.org). Secondary structures of RNAs were predicted using MFOLD (Zuker 2003).

Results

Sugar induction of *PAP1* and *TAS4* expression

PAP1 and PAP2 are predicted targets of *TAS4*-siR81(−) (Fig. 1a) (Rajagopalan et al. 2006). Using qRT-PCR, *PAP1* expression was assayed in response to sugars. In a time-course treatment with exogenous sugars of Col-0 seedlings, *PAP1* expression was induced by Suc and Glc up to ~5-and 14-fold, respectively, whereas *PAP1* was not induced by the non-

metabolizable sugar mannitol used as a control (Fig. 1b). *PAP2* showed a similar but lower induction than *PAP1* by Suc treatment (~6-fold less than *PAP1*; see Fig. 1c, the rows for "Ler-0" and "Col-0").

Abscisic acid (ABA) signaling synergizes with sugar and induces anthocyanin accumulation in early seedling development (Rolland et al. 2006; Finkelstein et al. 2002). Several sugar-insensitive mutants were isolated as allelic to *ABA synthesis* (*aba*) and *ABA insensitive* (*abi*) mutants. For example, *sucrose insensitive 10* (*sis10*) was cloned in a forward genetic screen and shown to be allelic to *ABI3*, encoding a B3 domain transcription factor that confers sugar and ABA sensitivity and regulates anthocyanin production (Parcy et al. 1997; Huang et al. 2008). *sucrose uncoupled 6 (sun6), sugar-insensitive 5 (sis5), glucose insensitive 6 (gin6)*, and *impaired sucrose induction 3 (isi3)* are mutant alleles of *ABI4*, which encodes an APETALA2 domain transcription factor (Huijser et al. 2000; Laby et al. 2000; Arenas-Huertero et al. 2000; Rook et al. 2001). To measure the effects of sugar induction on *PAP1* and *TAS4*, qRT-PCR assays were performed on samples from mutants in ABA biosynthesis and signaling pathways (Fig. 1c, d). Interestingly, in *abi1-1, abi2-1, abi4-103*, and *aba1-1* mutants the induction of *PAP1* and *PAP2* by Suc was significantly reduced (~2- to 8-fold) compared to wild type Ler-0 or Col-0, although still effectively Suc-responsive (Fig. 1c). This indicated the positive effect of ABA signaling and biosynthesis on *PAP1/PAP2* responses to Suc. In *abi3-1* and *abi5-1* mutants, *PAP1* expression upon Suc treatment was severely decreased compared to wild type (~21- and 47-fold less, respectively). In addition, *PAP2* barely responded to Suc treatment in *abi3-1* and *abi5-1* mutants. These results are generally consistent with the sugar-insensitive phenotypes associated with *abi3, abi4* and *abi5* mutants (Bossi et al. 2009). Interestingly, the expression of *MYB82*, a *PAP1* paralog which has a predicted but un-validated miR828 complementary site (Rajagopalan et al. 2006) (data not shown), did not respond to Suc in wild type or mutants. However, *TAS4* expression was increased two to threefold by Suc in the *abi1-1, abi3-1* and *abi5-1* mutants in comparison to Ler-0, suggesting its expression is independent of the ABA signaling pathway or subject to secondary effects (Fig. 1d).

sRNA blots showed that *TAS4*-siR81(−) was induced strongly in a dose-dependent manner by exogenous Suc treatment for 12 h (Fig. 2a). The expression of *TAS4*-siR81(−) was induced by physiological concentrations of 6.25 mM Suc or 12.5 mM Glc (Jang and Sheen 1994) relative to a corresponding control (2.1-, and 1.8-fold higher than mannitol control, respectively). Clear signals corresponding to *TAS4*-siR81(−) were detected for samples treated with 25 mM Suc (2.6-fold higher than that in samples treated by mannitol), with maximum signal intensities observed for samples treated with 100 mM Suc for 12 h (14-fold higher than mannitol control). Increasing Glc concentrations had similar effects as Suc on *TAS4*-siR81(−) expression (~3- to 6-fold induction after 12 h), while the non-metabolized osmolyte mannitol (a negative control) had a very weak effect, indicating that *TAS4*-siRNA81(−) induction is primarily due to metabolizable sugars and that the mannitol effect observed at high concentrations may be an osmotic stress-related response (Fig. 2a, data not shown). As the basis for quantifying endogenous sRNA abundance, miR160 and 5S rRNA expression were shown to be independent of sugar treatments, which supports the specificity of Suc and Glc induction for *TAS4*-siR81(−) expression (Fig. 2a, b). The response of *TAS4*-siR81(−) to Suc or Glc was also transient, reaching a peak at 12 h (~14- and 18-fold induction by Suc and Glc, respectively) with subsequent declines in abundance at 24 h (~6- and 4-fold induction by Suc or Glc, respectively, Fig. 2b), suggesting a homeostatic mechanism involving the expression of *TAS4*.

An autoregulatory feedback loop involving *PAP1* and *TAS4* regulates anthocyanin production

PAP1 is predicted to carry a functional *TAS4*-siR81(−) target site (Rajagopalan et al. 2006; Hsieh et al. 2009). Its regulation by RISC is supported by qRT-PCR experiments showing up-regulation in *mir828* and *tas4* T-DNA insertion mutants (Hsieh et al. 2009). We further examined the genetic requirements of *PAP1* induction in *ta*-siRNA pathway mutants, namely *dcl4-2, rdr6-15, sgs3-14*, and *hyl1-2*, in response to Suc. Fig. 3a (arrow) shows that *PAP1* mRNA was elevated from 2.6- to 10.7-fold in these mutant seedlings in response to treatment with sucrose for 12 h, as well as in *miR828* and *tas4* mutants (11.4- and 8.1-fold increases, respectively). In *pap1-D*, a dominant activation-tagged transgenic line, *PAP1* expression was elevated compared to wild type (5.8-fold induction). Interestingly, there was a band of size ~450 nt (asterisk in Fig. 3a) presumed to be the *TAS4*-siR81(−)-directed 3′ cleavage product of *PAP1* mRNA, based on similar phenomena observed for many miRNA targets (Souret et al. 2004). The cleavage product was just barely visible in Col-0, *dcl4-2*, and *hst-7*. The accumulation of both *PAP1* mRNAs and its 3′ cleavage product in *pap1-D* suggests that increased *PAP1* mRNA levels may enhance post-transcriptional regulation of itself by *TAS4*-siR81(−). A sRNA blot confirmed that *TAS4*-siR81(−) expression was below detection levels in wild type and all *ta*-siRNA pathway mutants assayed, but significantly increased in *pap1-D* (Fig. 3b). Taken together, these results suggest that an autoregulatory feedback loop involving *PAP1* and *TAS4*-siR81(−) operates on and coordinates *TAS4* expression. Supporting this notion, two putative PAP1-binding motifs (C/T)(A/C)NCCACNN(G/T) were found within the 2,000 nt region upstream of the *TAS4* transcription start site (Fig. S1A), according to PAP1 *cis*-regulatory elements functionally characterized by transient assays in protoplasts (Dare et al. 2008).

dcl4-2 and *drb4-1* mutants over-accumulate anthocyanin in leaves and flowers of plants older than 6 weeks (Nakazawa et al. 2007). To find out the effect of Suc treatments, we assayed the accumulation of anthocyanin in various *ta*-siRNA pathway mutants (Fig. 4). With the exception of *pap1-D*, untreated 3 day-old mutant seedlings did not accumulate significantly different amounts of anthocyanins than their corresponding wild types (Fig. 4, blue bars). After 12 h Suc treatment, all mutants displayed increased accumulation of anthocyanin compared to their non-treated seedlings (Fig. 4, red bars), consistent with previous findings (Nakazawa et al. 2007). Like untreated *pap1-D* mutant results, *pap1-D* seedlings had the highest anthocyanin accumulation after treatment, with *hyl1-2* mutants also accumulating significantly higher amounts of anthocyanins compared to wild type Col-0 (Fig. 4, asterisks). All other tested *ta*-siRNA pathway mutants accumulated higher amounts of anthocyanin than wild types. These results suggest that the release of *PAP1* repression by loss of *TAS4*-siR81(−) (Fig. 3a) in the mutants could be responsible for increased anthocyanin under Suc stimulus conditions (Fig. 4).

Evolution of *TAS4* and its regulator miR828

Bioinformatic analysis of ESTs in land plants demonstrated the existence of *TAS4* in dicots, such as *Euphorbia esula, Actinidia chinensis*, and *Vitis vinifera* (Fig. 5; data not shown). The *TAS4* orthologs bear conserved miR828 binding sites, whereas a less-conserved *TAS4*-siR81(−) complementary site is located downstream by a constant distance of four 21-nt phases (Fig. 5 black lines), despite the sequence divergence in the intervening region. These data clearly show that a “selective sweep” has acted over evolutionary time on miR828 and *TAS4*-siR81(−) sequences to maintain the function of *TAS4* in these species. Supporting evidence was found by alignment of sequences for PAP1/PAP2/MYB113 orthologs which show the peptide footprint for miR828 binding sites is generally conserved for both dicot and monocot plants (Fig. 6), while that for *TAS4*-siR81(−) binding sites is specific for most dicots only (Fig. 7). DNA sequence alignment revealed a MYB-like gene in Fagopyrum as

potential target for miR828, based on sequence similarity with miR828 complementary site in Arabidopsis *MYB113* (Fig. S2A). *MYBA6* in Vitis is also predicted as *TAS4* target (compare Fig. 5 with Fig. S2B; data not shown). These observations support purifying selection for miR828 and *TAS4* regulation on individual MYB targets in different dicot species as shown initially in Arabidopsis (Rajagopalan et al. 2006).

By searching plant EST databases, *MIR828* orthologs with extensive base pairing to form hairpins were found in a variety of dicot species, including *A. lyrata, E. esula, V. vinifera*, and gymnosperms *Picea glauca* (spruce) and *Pinus contorta* (lodgepole pine) (Fig. 8a and Figs. S3–S5). The candidate *MIR828s* share significant similarity for mature miR828 and flanking regions, suggesting an ancient origin of *MIR828* (Fig. 8a). Interestingly, genomic sequences with great similarity to the miR828 orthologs were found in *Trillium camschatcense* (Fig. 8a "Tca"), a basal monocot species. The *T. camschatcense* miR828-like sequence would form an extensive hairpin (a hallmark of miRNA precursors) if expressed (Fig. S6). In contrast to most monocots (which have characteristic narrow, thick, hard leaves with parallel venation and tiny, wind-dispersed seeds released from dry capsules), Trillium possesses broad, thin, soft leaves, net venation, and fleshy fruits (Givnish et al. 2006). This phylogenetic relationship suggests a plausible hypothesis that *MIR828* was lost early in the monocot lineage and plays some important roles in gymnosperm and dicot physiology. Remarkably, the gymnosperm *P. glauca* predicted pri-miR828 transcript carries two miR828 sites on a polycistronic precursor (Fig. S3), while all analyzed dicot pri-miR828s have one (Fig. S4, data not shown). Two predicted alternative secondary structures with similar delta-G free energies form "good" hairpin structure which could generate mature miR828 from either of these candidate loci (Fig. S3).

Sequence comparison among *MIR828, MYBs* and *TAS4* revealed some clues for a monophyletic origin. By DNA sequence alignment, extended similarities were found across the reverse strand of the *P. contorta* 5′ arm of *MIR828* precursor, the sense strand of the 3′ arm, and three predicted cognate *MYB* targets (Fig. 8b black line). Similarly, when the *A. thaliana TAS4* sequence is aligned with the arm for miR828* and its downstream sequences (presumably pri-miR828 sequence), they show extensive conservation, including and beyond the miR828 binding site (i.e. miR828*) and the region for the 3′ end of *TAS4* (Fig. 8c). Our data suggests an inverted duplication model for the evolution of *MIR828* and *TAS4* (see below).

To search for experimental evidence supporting our hypothesis for *TAS4* origin, a RACE assay was performed on RNA samples from ancient land plants, including *T. globosa* and *P. resinosa*. Using the conserved nucleotide sequence footprint found within miR828 binding sites for *TAS4* paralogs in dicot plants (Fig. 5), a degenerate primer was designed as described (Axtell and Bartel 2005). However, we were unsuccessful to clone any *TAS4* sequences (data not shown). Interestingly, MYB-like genes were cloned from these experiments which had plausible miR828 complementary sites (data not shown). Follow-up 5′-RACE experiments resulted in validation of cleaved products for the *P. resinosa MYB* gene at the putative miR828 binding site (Fig. 8d). Consistent with our model, no remnant *TAS4*-siR81(−) complementary site was found within this *MYB* cDNA sequence (GenBank accession no. HQ997774). These data support the existence of miR828 and a regulatory role in gymnosperms.

Discussion

PAP1 and *TAS4* respond to endogenous sugar signals

Based on the presented data, we propose a working model for the autoregulatory feedback loop involving *PAP1* and *TAS4* (Fig. 9). *PAP1/MYB75* expression is induced by exogenous

treatment of physiological concentrations of Suc and Glc in Arabidopsis seedlings. Suc may be transported into the nucleus by Suc transporter(s), which activates Suc-induced transcription factors that bind to the promoter of *PAP1* and activate its transcription (orange arrows). The elevated expression of PAP1 may bind to the promoter of *TAS4* via PAP1 *cis*-elements and promote the transcription of *TAS4. TAS4* may also respond to sugar stimulus through a signaling pathway in which PAP1 is involved. The subsequent increased expression of *TAS4* will produce more *TAS4*-siR81(−) by the guidance of miR828 through RISC-mediated cleavage, which then reduces the *PAP1* transcript level by the same mechanism (Fig. 9, scissors). The proper regulation of *PAP1* expression level by the autoregulatory feedback loop would give plants a means to monitor changes in nutrient and/or environmental conditions. Interestingly, *PAP1 cis*-regulatory elements are also found in the putative promoters for *MIR828* and *PAP1* itself (Fig. S1B&C), one of which may locate within the 3′-UTR of *FOREVER YOUNG* (*FEY*, AT4G27760), a gene upstream of *MIR828* (AT4G27765). This could suggest a complex transcriptional regulation by PAP1 on *TAS4, MIR828*, and itself.

Sugar sensing and signaling pathways have been tightly linked with P_i bioavailability in the root responding to P_i starvation (Hammond and White 2008). Arabidopsis plants accumulate starch and sugars in the leaves when treated with low P_i (Lundmark et al. 2010). Several phosphate starvation-responsive genes are sugar-inducible, including *PURPLE ACID PHOSPHATASE 17* (*PAP17/ACP5*), *RIBONUCLEASE 1* (*RNS1*), and *INDUCED BY PHOSPHATE STARVATION 1* (*IPS1*). On the other hand, some hexokinase-independent sugar-sensing genes, for example *β-AMYLASE* (*β-AMY*) and *CHALCONE SYNTHASE* (*CHS*), are induced by P_i starvation in detached leaf assays as well (Muller et al. 2005). Interestingly, *PAP1* expression is triggered by Suc treatment and P_i starvation to similar levels (4- and 3.5-fold, respectively) in a leaf transcriptome profiling study (Muller et al. 2007). miR828 and *TAS4*-siR81(−) expression respond to P_i deficiency in the shoots of Col-0 as shown by sRNA deep sequencing and Northern blot (Hsieh et al. 2009). However, this finding was not observed by other groups using either RT-PCR, sRNA sequencing, or locked nucleic acid-based microarrays (Pant et al. 2009; Lundmark et al. 2010).

It has been shown that Suc synthesis increases in the leaves of P_i-deficient Arabidopsis, bean, barley, spinach and soybean plants, although some variation may exist (Hammond and White 2008). Suc in the shoot can also be translocated to the root via phloem as the causal intermediary signal, supported by the evidence that Suc concentrations in the root of P_i-starved soybean plants are higher than that in P_i-replete plants (Fredeen et al. 1989; Ciereszko et al. 1996), but not in Arabidopsis (Ciereszko et al.2001). In addition, genetic screens identified a P_i-deficient mutant, *pho3*, with reduced root acid phosphatase activity under low P_i conditions (Zakhleniuk et al. 2001). *PHO3* is allelic to *SUC2*, a Suc transporter for phloem loading (Lloyd and Zakhleniuk 2004). The *pho3* mutants accumulate high levels of Suc and other carbohydrates because of its inability to translocate them to the roots. Strikingly, *PAP1* and *PAP2* expression is significantly increased in *pho3* mutants based on transcriptome profiling (Lloyd and Zakhleniuk 2004). Taken together, we propose that the up-regulation of *TAS4*-siR81(−) and miR828 in P_i deficiency could be the consequence of accumulation of Suc and/or Glc in the shoots. In line with this, *TAS4*-siR81(−) and miR828 are found in shoots, but not roots, of Col-0 seedlings under P_i starvation (Hsieh et al. 2009).

Evolution of *TAS* and *MIRNA* genes

We mapped the cleavage site on a MYB target guided by miR828 in *P. resinosa*, providing direct evidence for miR828 function in gymnosperms. Although *P. resinosa* miR828 was not found in this study, its paralogs were predicted in closely related *P. contorta* and *P. glauca* species with the same mature miR828 (Fig. 8a). It may indicate the conservation for miR828 sequence and for its regulation of MYB targets in gymnosperms. Interestingly, the

regulation of MYB expression in dicots may be different from that in gymnosperms. PAP1/PAP2/MYB113 in Arabidopsis all carry *TAS4*-siR81(−) binding site, and MYB113 is targeted by miR828 as well, which was confirmed by 5′-RACE (Rajagopalan et al. 2006). PAP1 and/or PAP2 are expressed more abundantly and widely than MYB113. For example, *PAP1* expression is induced by a variety of stress conditions such as heat, drought, chilling, N deficiency, and ABA in addition to sugars, whereby anthocyanin is accumulated [www.genevestigator.com (Hruz et al. 2008), data not shown]. The common availability of *TAS4*-siR81(−) binding sites in these MYBs could point out a more important role for *TAS4* regulation of them in dicots. miR828 may function as an upstream riboregulator for *MYBs*, in which it fine-tunes *TAS4* expression, whereas the downstream *TAS4*-derived siRNAs control *MYB* transcript levels. How miR828 and *TAS4* coordinates *MYB* expression in response to different physiological conditions becomes a critical question to answer.

Although the modes for generating *ta*-siRNAs and their functions in gene regulation and plant development have been extensively studied, little is known about the molecular evolution of *TAS* genes. The fact that miR828 and *TAS4*-siR81(−) regulate the same set of target genes provides a good case for phylogenetic analysis. From our bioinformatic approaches and RACE assays, *TAS4* paralogs are only found in dicot plants, while miR828 and its target orthologs are extant in gymnosperms and dicotyledonous plants, suggesting a more ancient origin for *MIR828*. The extended homologies of cognate *MIR828* with its targets in *P. contorta*, and for *TAS4* and *MIR828* 3′ arm with miR828* in Arabidopsis (Fig. 8b, c) may provide hints for an evolution pathway from *MIR828* to *TAS4*. Our hypothesis is that *MYB* sequences underwent inverted duplication in a common ancestor of gymnosperms and dicots, from which *MIR828* came into being. Subsequently, a duplication event may have occurred on the 3′ arm of miR828 to give two miR828* sequences. Such events could give birth to a proto *TAS4* gene, which would be captured by the *ta*-siRNA pathway(s). Superimposed evolutionary constraints may have driven it towards a role as a regulator of *MYB* gene expression. From the *MIR828*-like DNA sequence in *T. camschatcense* (Fig. 8a), we suggest *MIR828* sequences died early in the monocot lineage. The question of why we couldn't find any monocot or gymnosperm *TAS4* is unanswered, but may be related to evolution of specialized MYB functions with implications for homeostatic feedback regulation of environmental signals and the dicot radiation.

Supplementary Material

Refer to Web version on PubMed Central for supplementary material.

Acknowledgments

The authors thank the Arabidopsis Biological Resource Center at Ohio State University for seeds, the greenhouse staff in the Department of Biological Sciences at Texas Tech University, Ruth Finkelstein for the *abi4-103* mutant seeds, Zhixin Xie for the *rdr6-15* and *dcl4-2* mutant seeds, Xuemei Chen for the *hen1-1* mutant seeds, and Hong-Liang Zhu for discussion and technical support. This work was supported by the National Institutes of Health (R21GM077245 to C.D.R.)

References

Adenot X, Elmayan T, Lauressergues D, Boutet S, Bouche N, Gasciolli V, Vaucheret H. DRB4-dependent *TAS3 trans*-acting siRNAs control leaf morphology through AGO7. Curr Biol. 2006; 16:927–932. [PubMed: 16682354]

Allen E, Xie Z, Gustafson AM, Carrington JC. MicroRNA-directed phasing during *trans*-acting siRNA biogenesis in plants. Cell. 2005; 121:207–221. [PubMed: 15851028]

Alonso JM, Stepanova AN, Leisse TJ, Kim CJ, Chen H, Shinn P, Stevenson DK, Zimmerman J, Barajas P, Cheuk R, Gadrinab C, Heller C, Jeske A, Koesema E, Meyers CC, Parker H, Prednis L,

Ansari Y, Choy N, Deen H, Geralt M, Hazari N, Hom E, Karnes M, Mulholland C, Ndubaku R, Schmidt I, Guzman P, Aguilar-Henonin L, Schmid M, Weigel D, Carter DE, Marchand T, Risseeuw E, Brogden D, Zeko A, Crosby WL, Berry CC, Ecker JR. Genome-wide insertional mutagenesis of *Arabidopsis thaliana*. Science. 2003; 301:653–657. [PubMed: 12893945]

Arenas-Huertero F, Arroyo A, Zhou L, Sheen J, Leon P. Analysis of *Arabidopsis* glucose insensitive mutants, *gin5* and *gin6*, reveals a central role of the plant hormone ABA in the regulation of plant vegetative development by sugar. Genes Dev. 2000; 14:2085–2096. [PubMed: 10950871]

Axtell MJ, Bartel DP. Antiquity of microRNAs and their targets in land plants. Plant Cell. 2005; 17:1658–1673. [PubMed: 15849273]

Borevitz JO, Xia Y, Blount J, Dixon RA, Lamb C. Activation tagging identifies a conserved MYB regulator of phenylpropanoid biosynthesis. Plant Cell. 2000; 12:2383–2394. [PubMed: 11148285]

Bossi F, Cordoba E, Dupre P, Mendoza MS, Roman CS, Leon P. The Arabidopsis ABA-Insensitive (ABI) 4 factor acts as a central transcription activator of the expression of its own gene, and for the induction of ABI5 and SBE2.2 genes during sugar signaling. Plant J. 2009; 59:359–374. [PubMed: 19392689]

Chang S, Puryear J, Cairney J. A simple and efficient method for isolating RNA from pine trees. Plant Mol Biol Rep. 1993; 11:113–116.

Chiou TJ, Aung K, Lin SI, Wu CC, Chiang SF, Su CL. Regulation of phosphate homeostasis by microRNA in Arabidopsis. Plant Cell. 2006; 18:412–421. [PubMed: 16387831]

Ciereszko IGA, Mikulska M, Rychter AM. Assimilate translocation in bean plants (*Phaseolus vulgaris* l.) during phosphate deficiency. J Plant Physiol. 1996; 149:343–348.

Ciereszko I, Johansson H, Hurry V, Kleczkowski LA. Phosphate status affects the gene expression, protein content and enzymatic activity of UDP-glucose pyrophosphorylase in wild-type and *pho* mutants of *Arabidopsis*. Planta. 2001; 212:598–605. [PubMed: 11525517]

Dare AP, Schaffer RJ, Lin-Wang K, Allan AC, Hellens RP. Identification of a *cis*-regulatory element by transient analysis of co-ordinately regulated genes. Plant Methods. 2008; 4:17. [PubMed: 18601751]

Dugas DV, Bartel B. Sucrose induction of *Arabidopsis* miR398 represses two Cu/Zn superoxide dismutases. Plant Mol Biol. 2008; 67:403–417. [PubMed: 18392778]

Fahlgren N, Montgomery TA, Howell MD, Allen E, Dvorak SK, Alexander AL, Carrington JC. Regulation of auxin response Factor3 by *TAS3 ta*-siRNA affects developmental timing and patterning in *Arabidopsis*. Curr Biol. 2006; 16:939–944. [PubMed: 16682356]

Finkelstein RR, Gampala SS, Rock CD. Abscisic acid signaling in seeds and seedlings. Plant Cell. 2002; 14(Suppl):S15–S45. [PubMed: 12045268]

Franco-Zorrilla JM, Valli A, Todesco M, Mateos I, Puga MI, Rubio-Somoza I, Leyva A, Weigel D, Garcia JA, Paz-Ares J. Target mimicry provides a new mechanism for regulation of microRNA activity. Nat Genet. 2007; 39:1033–1037. [PubMed: 17643101]

Fredeen AL, Rao IM, Terry N. Influence of phosphorus nutrition on growth and carbon partitioning in *Glycine max*. Plant Physiol. 1989; 89:225–230. [PubMed: 16666518]

Fujii H, Chiou TJ, Lin SI, Aung K, Zhu JK. A miRNA involved in phosphate-starvation response in *Arabidopsis*. Curr Biol. 2005; 15:2038–2043. [PubMed: 16303564]

Garcia D, Collier SA, Byrne ME, Martienssen RA. Specification of leaf polarity in *Arabidopsis* via the *trans*-acting siRNA pathway. Curr Biol. 2006; 16:933–938. [PubMed: 16682355]

Givnish TJ, Pires JC, Graham SW, Mcpherson MA, Prince LM, Patterson TB, Rai HS, Roalson EH, Evans TM, Hahn WJ, Millam KC, Meerow AW, Molvray M, Kores PJ, O'brien HE, Hall JC, Kress WJ, Sytsma KJ. Phylogenetic relationships of monocots based on the highly informative plastid gene *ndhF*: evidence for widespread concerted convergence. Aliso. 2006; 22:28–51.

Gonzalez A, Zhao M, Leavitt JM, Lloyd AM. Regulation of the anthocyanin biosynthetic pathway by the TTG1/BHLH/MYB transcriptional complex in *Arabidopsis* seedlings. Plant J. 2008; 53:814–827. [PubMed: 18036197]

Hammond JP, White PJ. Sucrose transport in the phloem: integrating root responses to phosphorus starvation. J Exp Bot. 2008; 59:93–109. [PubMed: 18212031]

Higo K, Ugawa Y, Iwamoto M, Korenaga T. Plant *cis*-acting regulatory DNA elements (PLACE) database. Nucleic Acids Res. 1999; 27:297–300. [PubMed: 9847208]

Hruz T, Laule O, Szabo G, Wessendorp F, Bleuler S, Oertle L, Widmayer P, Gruissem W, Zimmermann P. Genevestigator v3: A reference expression database for the meta-analysis of transcriptomes. Adv Bioinform. 2008; 2008:420747.

Hsieh LC, Lin SI, Shih AC, Chen JW, Lin WY, Tseng CY, Li WH, Chiou TJ. Uncovering small RNA-mediated responses to phosphate deficiency in *Arabidopsis* by deep sequencing. Plant Physiol. 2009; 151:2120–2132. [PubMed: 19854858]

Huang Y, Li CY, Biddle KD, Gibson SI. Identification, cloning and characterization of *sis7* and *sis10* sugar-insensitive mutants of *Arabidopsis*. BMC Plant Biol. 2008; 8:104. [PubMed: 18854047]

Huijser C, Kortstee A, Pego J, Weisbeek P, Wisman E, Smeekens S. The Arabidopsis *SUCROSE UNCOUPLED-6* gene is identical to *ABSCISIC ACID INSENSITIVE-4*: involvement of abscisic acid in sugar responses. Plant J. 2000; 23:577–585. [PubMed: 10972884]

Jang JC, Sheen J. Sugar sensing in higher plants. Plant Cell. 1994; 6:1665–1679. [PubMed: 7827498]

Jones-Rhoades MW, Bartel DP. Computational identification of plant microRNAs and their targets, including a stress-induced miRNA. Mol Cell. 2004; 14:787–799. [PubMed: 15200956]

Kawashima CG, Yoshimoto N, Maruyama-Nakashita A, Tsuchiya YN, Saito K, Takahashi H, Dalmay T. Sulphur starvation induces the expression of microRNA-395 and one of its target genes but in different cell types. Plant J. 2009; 57:313–321. [PubMed: 18801012]

Laby RJ, Kincaid MS, Kim D, Gibson SI. The *Arabidopsis* sugar-insensitive mutants *sis4* and *sis5* are defective in abscisic acid synthesis and response. Plant J. 2000; 23:587–596. [PubMed: 10972885]

Lloyd JC, Zakhleniuk OV. Responses of primary and secondary metabolism to sugar accumulation revealed by microarray expression analysis of the *Arabidopsis* mutant, *pho3*. J Exp Bot. 2004; 55:1221–1230. [PubMed: 15133053]

Lundmark M, Korner CJ, Nielsen TH. Global analysis of microRNA in *Arabidopsis* in response to phosphate starvation as studied by locked nucleic acid-based microarrays. Physiol Plant. 2010; 140:57–68. [PubMed: 20487378]

Luo QJ, Samanta MP, Koksal F, Janda J, Galbraith DW, Richardson CR, Ou-Yang F, Rock CD. Evidence for antisense transcription associated with microRNA target mRNAs in *Arabidopsis*. PLoS Genet. 2009; 5(4):e1000457. [PubMed: 19381263]

Marin E, Jouannet V, Herz A, Lokerse AS, Weijers D, Vaucheret H, Nussaume L, Crespi MD, Maizel A. miR390, *Arabidopsis TAS3* tasiRNAs, and their auxin response factor targets define an autoregulatory network quantitatively regulating lateral root growth. Plant Cell. 2010; 22:1104–1117. [PubMed: 20363771]

Montgomery TA, Howell MD, Cuperus JT, Li D, Hansen JE, Alexander AL, Chapman EJ, Fahlgren N, Allen E, Carrington JC. Specificity of Argonaute7-miR390 interaction and dual functionality in *TAS3 trans*-acting siRNA formation. Cell. 2008a; 133:128–141. [PubMed: 18342362]

Montgomery TA, Yoo SJ, Fahlgren N, Gilbert SD, Howell MD, Sullivan CM, Alexander A, Nguyen G, Allen E, Ahn JH, Carrington JC. AGO1-miR173 complex initiates phased siRNA formation in plants. Proc Natl Acad Sci USA. 2008b; 105:20055–20062. [PubMed: 19066226]

Muller R, Nilsson L, Nielsen LK, Nielsen TH. Interaction between phosphate starvation signalling and hexokinase-independent sugar sensing in *Arabidopsis* leaves. Physiol Plant. 2005; 124:81–90.

Muller R, Morant M, Jarmer H, Nilsson L, Nielsen TH. Genome-wide analysis of the Arabidopsis leaf transcriptome reveals interaction of phosphate and sugar metabolism. Plant Physiol. 2007; 143:156–171. [PubMed: 17085508]

Nakazawa Y, Hiraguri A, Moriyama H, Fukuhara T. The dsRNA-binding protein DRB4 interacts with the Dicer-like protein DCL4 in vivo and functions in the *trans*-acting siRNA pathway. Plant Mol Biol. 2007; 63:777–785. [PubMed: 17221360]

Pant BD, Musialak-Lange M, Nuc P, May P, Buhtz A, Kehr J, Walther D, Scheible WR. Identification of nutrient-responsive *Arabidopsis* and rapeseed microRNAs by comprehensive real-time polymerase chain reaction profiling and small RNA sequencing. Plant Physiol. 2009; 150:1541–1555. [PubMed: 19465578]

Parcy F, Valon C, Kohara A, Misera S, Giraudat J. The *ABSCISIC ACID-INSENSITIVE3, FUSCA3*, and *LEAFY COTYLEDON1* loci act in concert to control multiple aspects of *Arabidopsis* seed development. Plant Cell. 1997; 9:1265–1277. [PubMed: 9286105]

Peragine A, Yoshikawa M, Wu G, Albrecht HL, Poethig RS. *SGS3* and *SGS2/SDE1/RDR6* are required for juvenile development and the production of *trans*-acting siRNAs in *Arabidopsis*. Genes Dev. 2004; 18:2368–2379. [PubMed: 15466488]

Pourtau N, Jennings R, Pelzer E, Pallas J, Wingler A. Effect of sugar-induced senescence on gene expression and implications for the regulation of senescence in *Arabidopsis*. Planta. 2006; 224:556–568. [PubMed: 16514542]

Rajagopalan R, Vaucheret H, Trejo J, Bartel DP. A diverse and evolutionarily fluid set of microRNAs in *Arabidopsis thaliana*. Genes Dev. 2006; 20:3407–3425. [PubMed: 17182867]

Rolland F, Baena-Gonzalez E, Sheen J. Sugar sensing and signaling in plants: conserved and novel mechanisms. Ann Rev Plant Biol. 2006; 57:675–709. [PubMed: 16669778]

Rook F, Corke F, Card R, Munz G, Smith C, Bevan MW. *Impaired sucrose-induction* mutants reveal the modulation of sugar-induced starch biosynthetic gene expression by abscisic acid signalling. Plant J. 2001; 26:421–433. [PubMed: 11439129]

Solfanelli C, Poggi A, Loreti E, Alpi A, Perata P. Sucrose-specific induction of the anthocyanin biosynthetic pathway in Arabidopsis. Plant Physiol. 2006; 140:637–646. [PubMed: 16384906]

Souret FF, Kastenmayer JP, Green PJ. AtXRN4 degrades mRNA in *Arabidopsis* and its substrates include selected miRNA targets. Mol Cell. 2004; 15:173–183. [PubMed: 15260969]

Teng S, Keurentjes J, Bentsink L, Koornneef M, Smeekens S. Sucrose-specific induction of anthocyanin biosynthesis in *Arabidopsis* requires the *MYB75/PAP1* gene. Plant Physiol. 2005; 139:1840–1852. [PubMed: 16299184]

Vazquez F, Vaucheret H, Rajagopalan R, Lepers C, Gasciolli V, Mallory AC, Hilbert JL, Bartel DP, Crete P. Endogenous *trans*-acting siRNAs regulate the accumulation of *Arabidopsis* mRNAs. Mol Cell. 2004; 16:69–79. [PubMed: 15469823]

Xie Z, Allen E, Wilken A, Carrington JC. DICER-like 4 functions in *trans*-acting small interfering RNA biogenesis and vegetative phase change in *Arabidopsis thaliana*. Proc Natl Acad Sci USA. 2005; 102:12984–12989. [PubMed: 16129836]

Yoon EK, Yang JH, Lim J, Kim SH, Kim SK, Lee WS. Auxin regulation of the microRNA390-dependent transacting small interfering RNA pathway in Arabidopsis lateral root development. Nucleic Acids Res. 2010; 38:1382–1391. [PubMed: 19969544]

Yoshikawa M, Peragine A, Park MY, Poethig RS. A pathway for the biogenesis of *trans*-acting siRNAs in *Arabidopsis*. Genes Dev. 2005; 19:2164–2175. [PubMed: 16131612]

Zakhleniuk OV, Raines CA, Lloyd JC. *pho3*: A phosphorus-deficient mutant of *Arabidopsis thaliana* (L. Heynh). Planta. 2001; 212:529–534. [PubMed: 11525509]

Zuker M. MFold web server for nucleic acid folding and hybridization prediction. Nucleic Acids Res. 2003; 31:3406–3415. [PubMed: 12824337]

Abbreviations

TAS	*Trans-Acting SiRNA Gene*
miRNA	microRNA
Suc	Sucrose
Glc	Glucose
PAP1	Production of Anthocyanin Pigment1
qRT-PCR	Quantitative real-time Polymerase Chain Reaction
ABA	Abscisic acid
sRNA	Small RNA

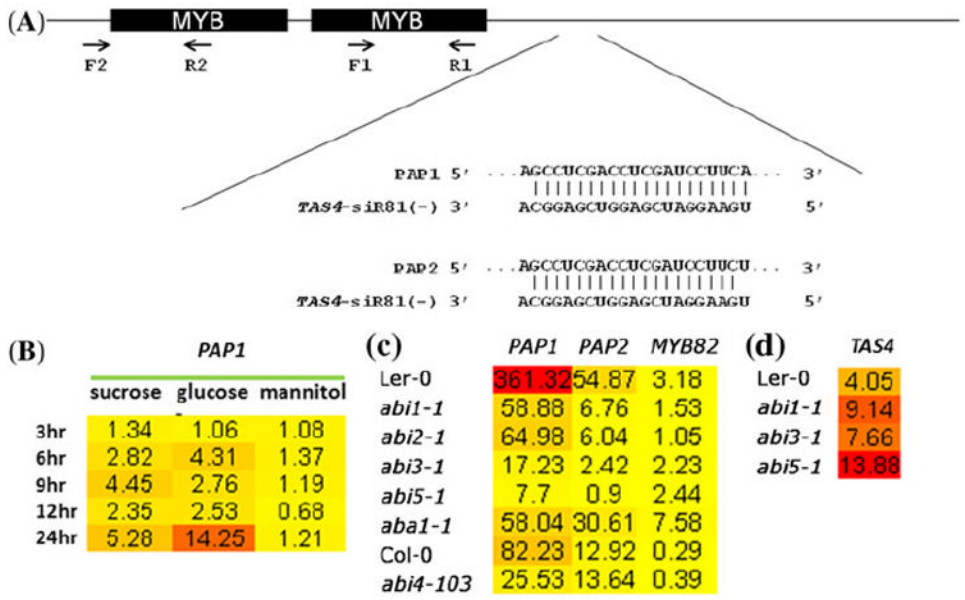

Fig. 1.

qRT-PCR shows temporal induction of *PAP1, PAP2* and *TAS4* by Suc and Glc, and crosstalk with ABA signaling. Panel **a** schematic of *PAP1* and *PAP2* genes with qRT-PCR primer pairs mapped below (F1, R1 for *PAP1*; F2, R2 for *PAP2*, respectively). The base pairing between *TAS4*-siR81(−) with PAP1 or PAP2 is shown underneath. Panel **b** Time course of Suc, Glc, or mannitol treatments of Col-0 seedling at a concentration of 100 mM up to 24 h. Each treatment is represented by a column of *colored boxes*, and each time point is indicated by an individual row. For Suc treatment of Arabidopsis seedlings, 3-day-old seedlings were grown on filter papers supplemented with Murashige and Skoog (*MS*) standard medium (½ strength, control). Data (average transcript level from three technical replicates) were visualized using BAR HeatMapper Plus software (http://bar.utoronto.ca/ntools/cgi-bin/ntools_heatmapper_plus.cgi). Data are represented as fold change (unity = control) after normalization to *ACTIN8* expression. Effects of different sugars on gene expression range from *pale yellow* (low) to *deep red* (high). The experiment was performed twice with similar results. Panels **c, d** 100 mM Suc response of ABA mutant genotypes treated for 24 h. The expression data for each gene is represented by a column of *colored boxes*, while each genotype assayed is indicated by an *individual row*

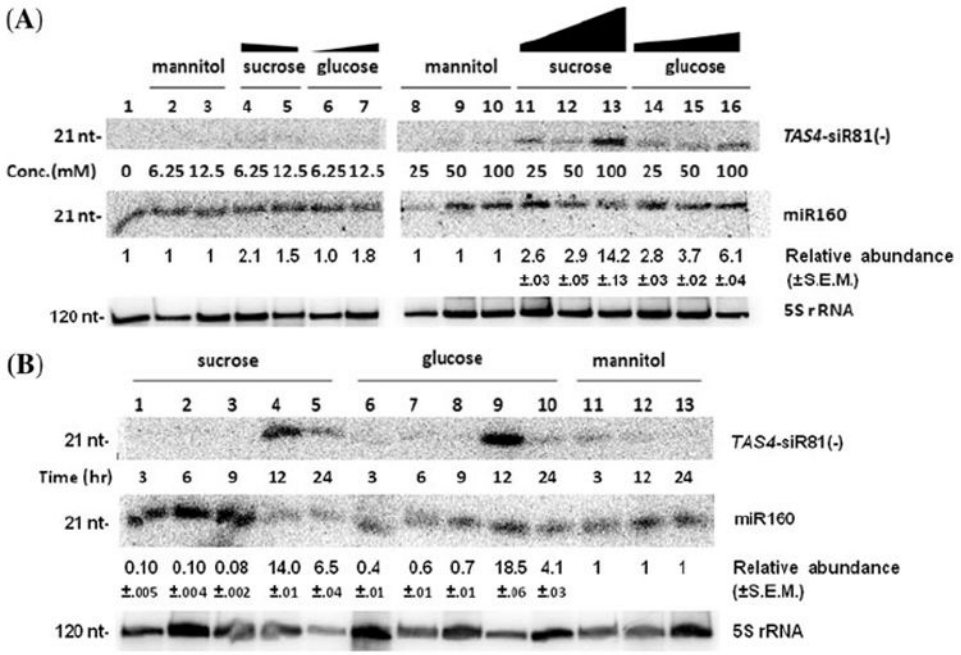

Fig. 2.

Physiological concentrations of Suc and Glc induce expression of *TAS4*-siR81(−). Panel **a** 3-day-old Col-0 wild-type seedlings were grown on filter papers supplemented with MS medium (½ strength, control) and then subjected to treatment with different sugars in series of concentrations ranging from 0 to 100 mM for 12 h. Panel **b** time-course experiment from 3 to 24 h treatments with 100 mM Suc, Glc or mannitol. As loading controls, probes for 5S rRNA and miR160 were hybridized to the same membrane. Band intensities for *TAS4*-siR81(−) are shown normalized to that of miR160 below each lane (±standard error of mean) and graphically as 'effect wedges' above the treatment headers. The relative abundances for *TAS4*-siR81(−) are presented as the ratio of normalized abundance from Suc or Glc treatments to that from respective mannitol controls (set to unity). A representative result from three experiments is shown

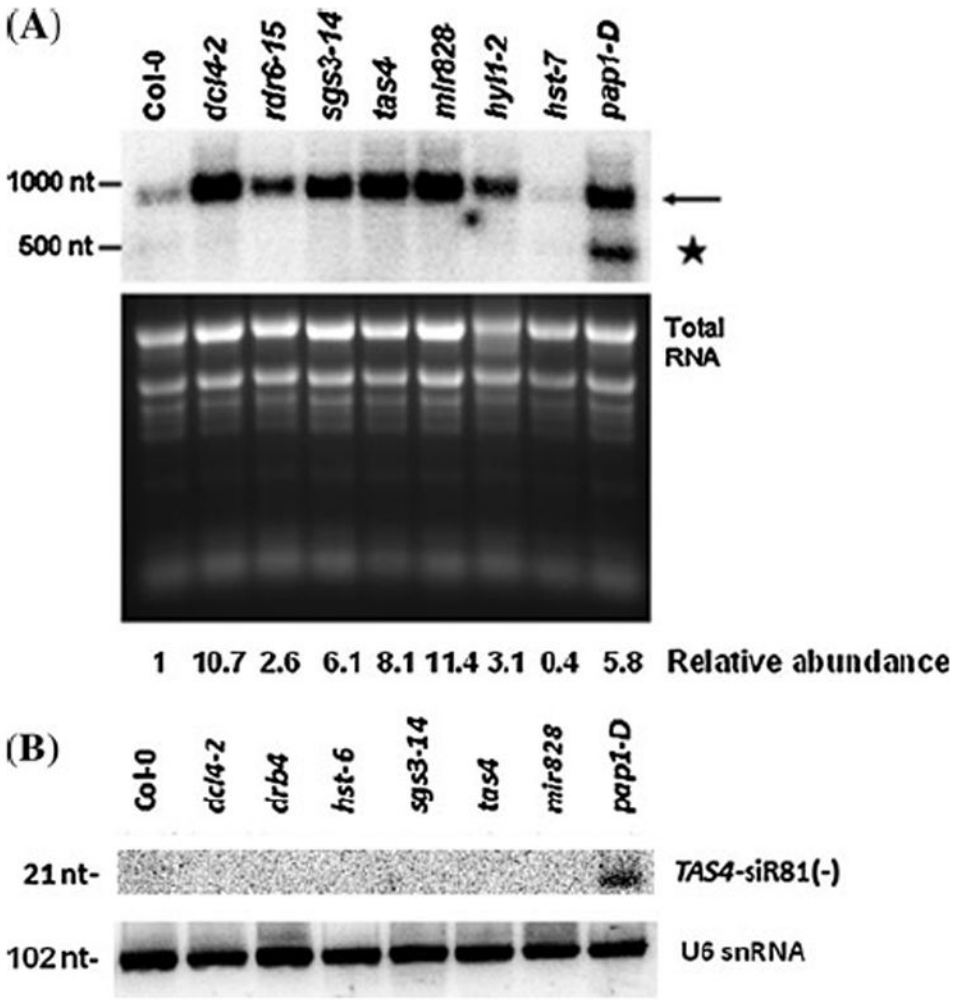

Fig. 3.

a negative feedback regulatory loop involving with *PAP1* and *TAS4*-siR81(−). Panel **a** 3-day-old Col-0 wild-type seedlings were grown on filter papers supplemented with ½ strength MS medium (control) and then subjected to treatment with 100 mM sucrose for 12 h. The *arrow* indicates a band corresponding to the full length mRNA for *PAP1*, and the *star* shows a signal with the correct predicted size of the *TAS4*-siR81(−)-mediated 3′ cleavage product of *PAP1*. Total RNA (10 μg) was loaded for each sample and stained with ethidium bromide before blotting to confirm equal loadings. The relative abundance for *PAP1* is presented below the gel as the ratio of band intensities for each mutant versus that from wild type Col-0. Panel **b** sRNA blot analysis for *TAS4*-siR81(−) expression in *ta*-siRNA pathway mutants, a *mir828* T-DNA insertion mutant, and a *pap1-D* over-expressing activation-tagged transgenic line. Low molecular weight RNA (20 μg) was loaded for *each lane*. The same membrane was re-hybridized with a probe against U6 snRNA to show equal loading. The experiment was repeated twice with similar results

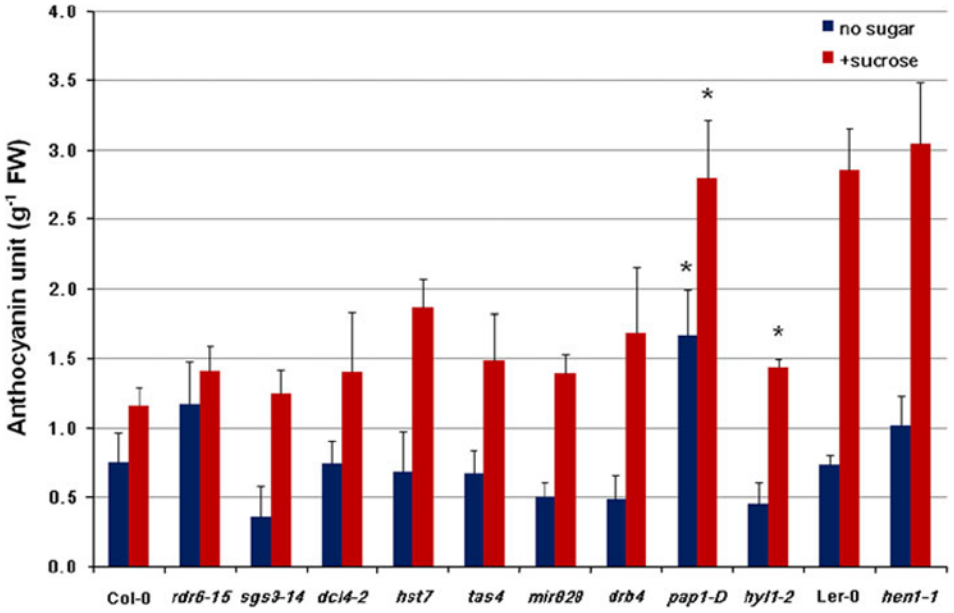

Fig. 4.

Sucrose treatment induces anthocyanin accumulation in *ta*-siRNA pathway mutants. Three-day-old Arabidopsis seedlings were grown on filter papers supplemented with MS medium (½ strength), half of which were transferred to new filter papers supplemented with 100 mM Suc for 12 h and the rest treated with H_2O. Data from one of two representative experiments is shown. *Error bars* are standard errors of mean ($n = 3$ biological replicates). *Asterisks* indicate significantly higher anthocyanin than wild type control ($P < 0.06$, one-sided Student's t-test, equal variance assumed)

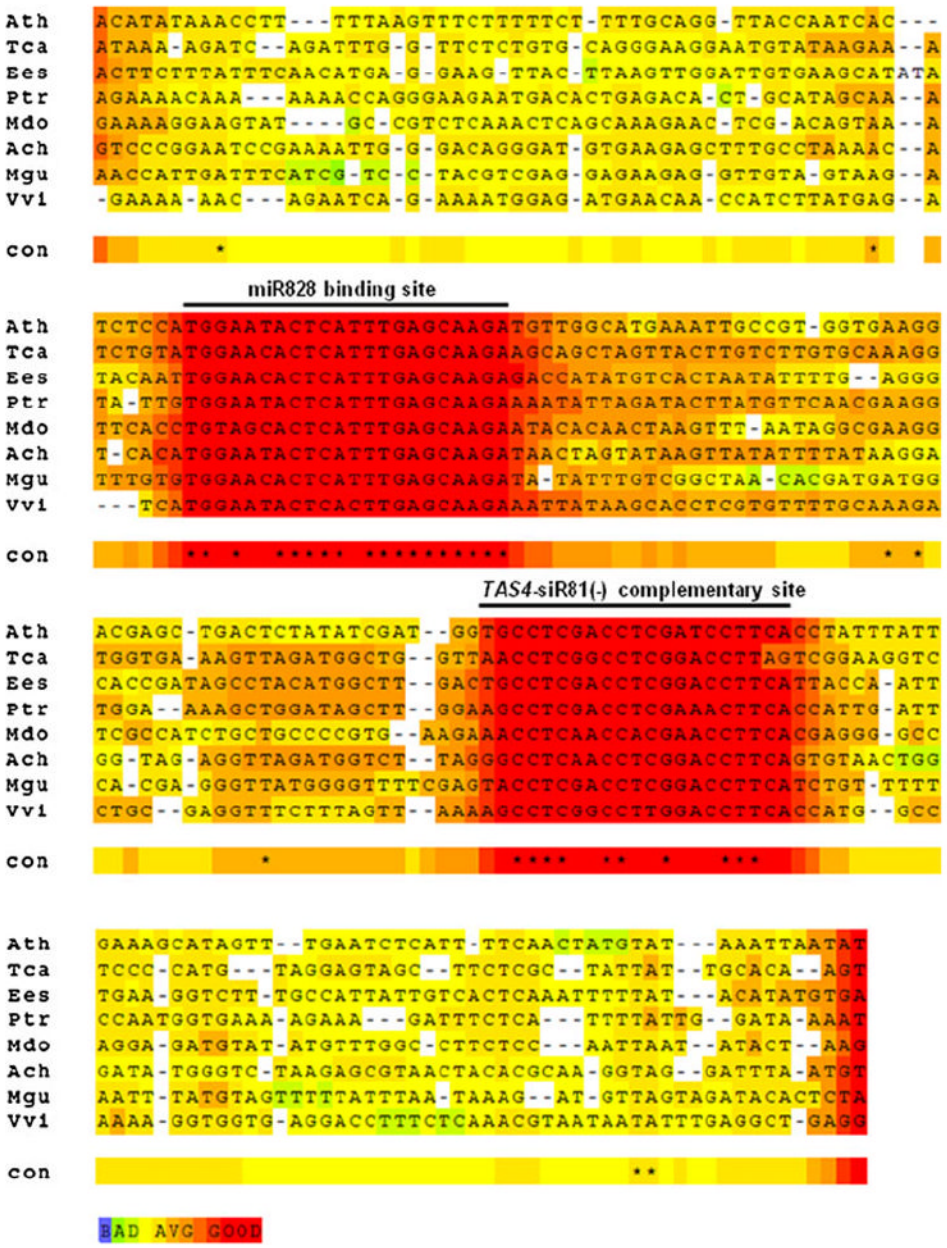

Fig. 5.

Sequence alignment of *TAS4* paralogs in dicot plants. Sequences were obtained by BLASTing *TAS4/AT3G25795* (n.t. 870–980) against the GenBank experimental plant EST database. Alignments were color-coded based on the confidence of the local alignment of T-Coffee (yellow < brown < red, www.tcoffee.org). The putative miR828 binding site and *TAS4*-siR81(−)-generating site are labeled with *black lines*. *Asterisks* show residues identical for the given position. Abbreviations correspond to species are listed as follows with *TAS4* paralog (GenBank accession numbers). Ath, *Arabidopsis thaliana*; Tca, *Theobroma cacao* (CU512683.1); Ees, *Euphorbia esula* (DV114602.1); Ptr, *Populus tremula* (DN495932.1); Mdo, *Malus domestica* (CN490819.1); Ach, *Actinidia chinensis* (FG511890.1); Mgu, *Mimulus guttatus* (DV209191.1), and Vvi, *Vitis vinifera*

(EC986896.1). *Con* consensus, the same nucleotide on one position is represented by *asterisk*

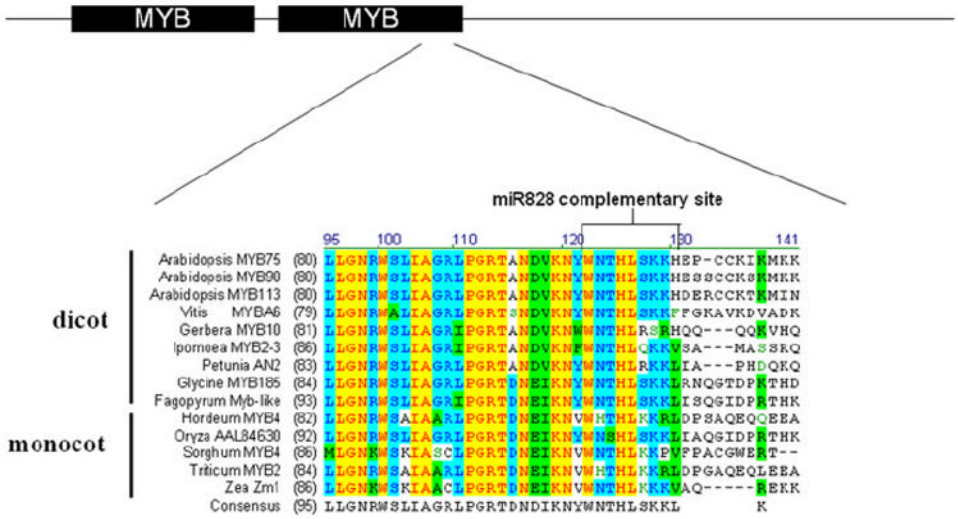

Fig. 6.

Amino acid sequence alignment of miR828 complementary sites in PAP1 orthologs from diverse flowering plant genera. Sequences were obtained by BLASTing the Arabidopsis PAP1 sequence to the GenBank protein database (www.ncbi.nlm.nih.gov). The alignment was done by Vector NTI (Invitrogen, version 9). A cartoon for MYB ortholog conserved domain structure is shown above the alignment. The miR828 complimentary sites are labeled by a bracket and the conserved residues are *shaded*

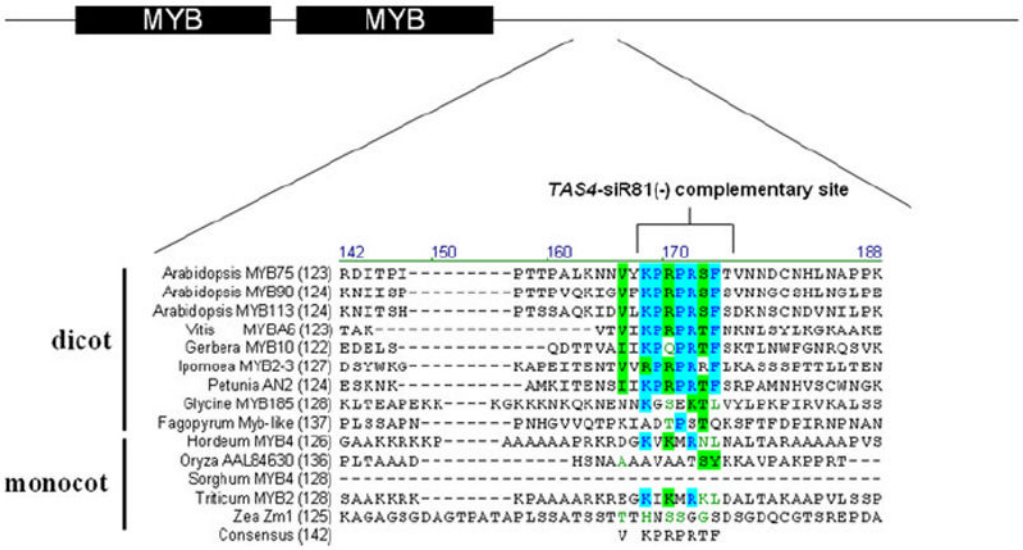

Fig. 7.

Amino acid sequence alignment of *TAS4*-siR81(−) complementary sites in PAP1 orthologs from diverse flowering plant genera. See legend of Fig. 6 for details of methods

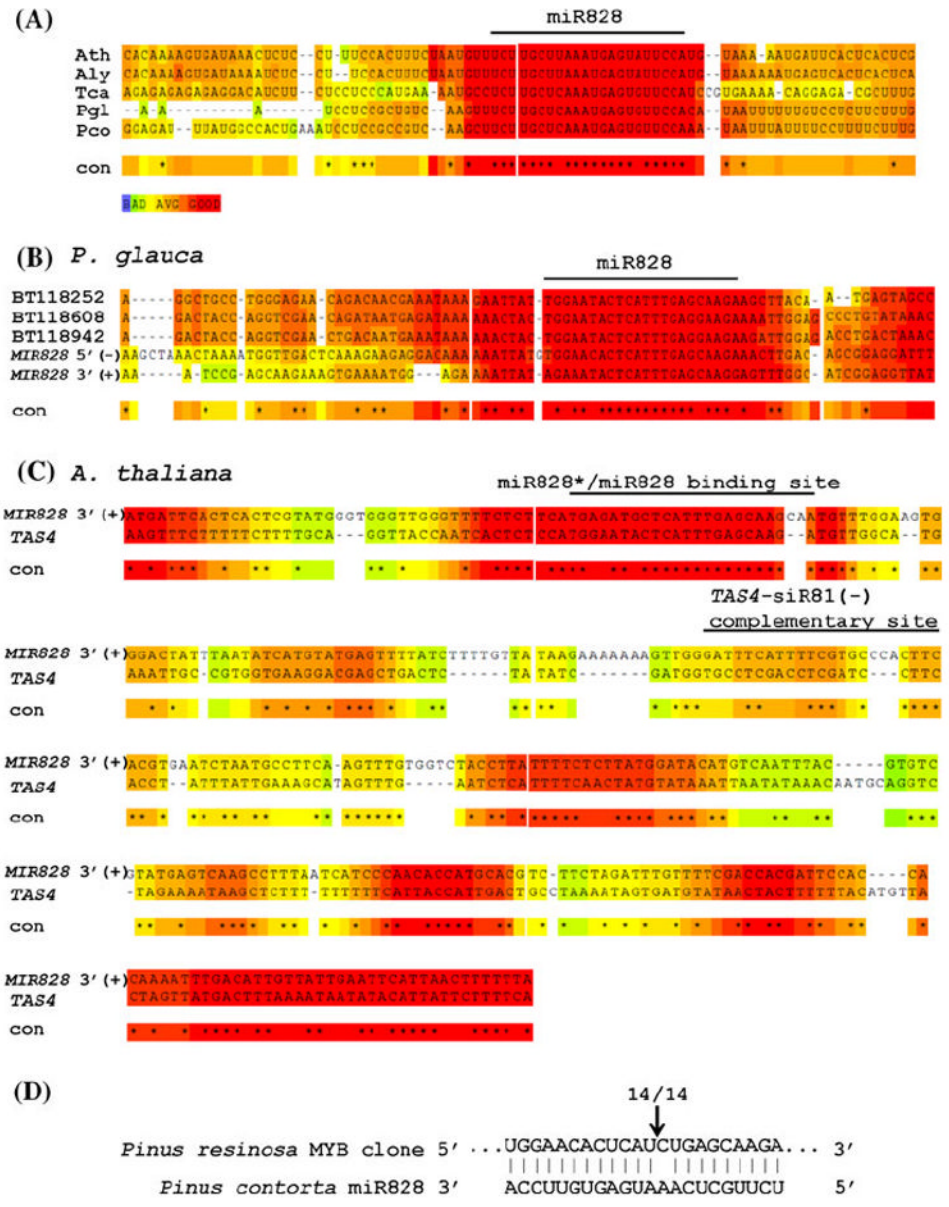

Fig. 8.

Evolution and function of *MIR828* and *TAS4* evidenced by sequence alignment and modified 5’-RACE validation of MYB endonucleolytic cleavage in a gymnosperm. Panel **a** Sequence alignment for *MIR828* genes from dicot, monocot and gymnosperm species. Alignments were color-coded based on the confidence of the local alignment of T-Coffee (yellow < brown < red). The predicted mature miR828 sites are labeled with a *black line. Asterisks* show consensus (con) nucleotides identical for the given position. Abbreviations correspond to species listed as follows (with accession numbers from GenBank). Arabidopsis *MIR828* sequences are from miRBase. In *Picea glauca*, since there are two miR828 sequences on one long precursor, sequences spanning the 5’ mature miR828 is used for alignment. Ath, *A. thaliana*; Aly, *Arabidopsis lyrata*; Tca, *Trillium camschatcense* (AB250300.1); Pgl, *Picea glauca* (CO236109.1); Pco, *Pinus contorta* (GT251244.1). Panel **b** extended sequence alignment of candidate *P. contorta MIR828* gene and three predicted *MYB* targets from *P. contorta*. The GenBank accession numbers for *MYB* targets are

shown. *MIR828* 5' arm (−) is the reverse complement sequence for the strand where mature miR828 locates. *MIR828* 3' arm (+) is the strand where miR828* maps. The location corresponding to mature miR828 is labeled by a *black line*. Panel **c** sequence alignment for *MIR828* gene and *TAS4* in *A. thaliana* showing homologies suggestive of a common evolutionary lineage. The miR828* site on the *MIR828* 3′ arm (+) and the miR828 and siR81(−) complementary sites on *TAS4* are indicated by *black lines*. Panel **d** 5′-RACE clones establish cleavage of a *P. resinosa MYB* target mRNA by miR828. All 14 clones sequenced mapped to the predicted miR828-cleavage site, based on the closely related *P. contorta* miR828

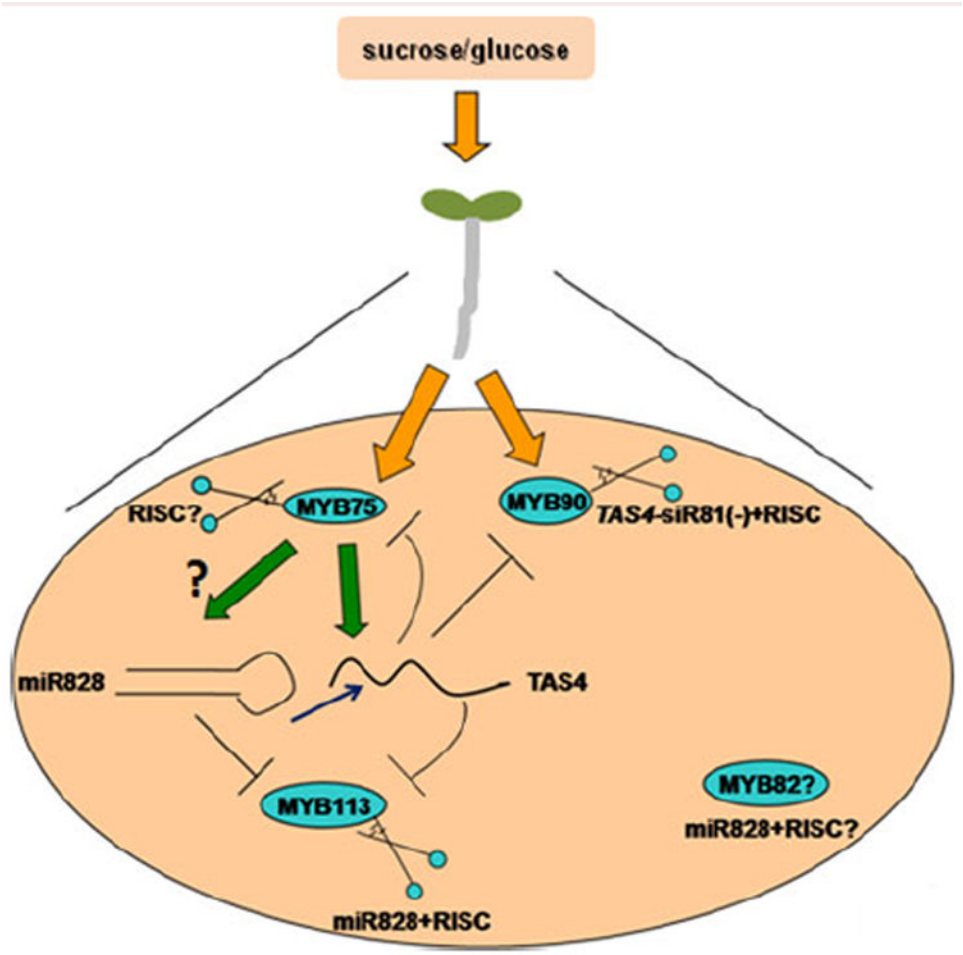

Fig. 9.

A working model for the feedback regulatory loop involving *PAP1/MYB75* and *TAS4* in response to sugars in Arabidopsis. *PAP1* expression is induced by Suc, Glc or other stimulus. PAP1 may regulate *TAS4* expression presumably by binding to the PAP1 *cis*-regulatory elements in *TAS4* promoter and transactivate its transcription. Alternatively, *TAS4* expression may directly respond to sugar stimulus through a signaling pathway involving PAP1. Increased *TAS4* transcript abundance generates more *TAS4*-siR81(−) through the *ta*-siRNA pathway, which then down-regulates *PAP1, PAP2* and *MYB113* expression levels. miR828 controls *MYB113* expression by guiding *MYB113* transcripts into RISC. At the same time, miR828 also promotes *TAS4* cleavage and routes its cleaved product into *ta*-siRNA pathways for *TAS4*-siR81(−) biogenesis, which reinforces the feedback loop involving *PAP1* and *TAS4*, as well as the regulatory network on PAP2 and MYB113 by *TAS4*. It is not clear whether PAP1 regulates *MIR828* transcription, or whether miR828 can down-regulate the expression level of *MYB82*, a putative miR828 target